Rao and Venkateshwarlu
Journal of Engineering and Applied Science (2024) 71:49
https://doi.org/10.1186/s44147-024-00384-z

Journal of Engineering and Applied Science

RESEARCH Open Access

Soft-switching dual active bridge converter-based bidirectional on-board charger for electric vehicles under vehicle-to-grid and grid-to-vehicle control optimization

J. V. G. Rama Rao[1*] and S. Venkateshwarlu[2]

*Correspondence:
jvgramarao2@gmail.com

[1] Department of Electrical and Electronics Engineering, BVC Institute of Technology and Science, Amalapuram 533221, India
[2] Department of Electrical Engineering, CVR College of Engineering, Ibrahimpatnam 501510, India

Abstract

Electric vehicles (EVs) are rapidly replacing conventional fuel vehicles, offering powerful, emission-free performance. This paper introduces an innovative three-phase bidirectional charger for grid-to-vehicle (G2V) and vehicle-to-grid (V2G) applications, strengthening the connection between EVs and the power grid. The charger employs a two-stage power conversion approach with advanced converters and a simplified dq-based charging control strategy. An efficient AC-DC converter facilitates smooth transitions between modes, responding to grid directives for active and reactive power. A soft-switching dual active bridge (SS-DAB) DC-DC converter optimally interfaces with the EV battery pack, while dual active LCL filters suppress harmonics, enhancing system performance. Simulated results confirm the charger's effectiveness in a 3.5-kW prototype using MATLAB/Simulink. The proposed SS-DAB converter-based bidirectional on-board charger introduces a groundbreaking unified Voltage Source Converter (VSC) control approach, enabling efficient power transfer in both vehicle-to-grid (V2G) and grid-to-vehicle (G2V) modes. This innovation ensures rapid dynamic response, exceptional steady-state performance, and robustness against grid demand changes, optimizing EV integration.

Keywords: Charging control, Distribution networks, Electric vehicle (EV), EV charger modeling, Smart battery charger, Vehicle-to-grid (V2G)

Introduction

Motivation and incitement

The shortage of energy and environmental consciousness has increased the production of automobiles, according to the research. Over their lifetime, EVs reduce emissions by 47%. At high fuel prices, EVs reduce energy consumption and emissions, but initial expenses could exceed advancements [1, 2]. Numerous research studies are looking for real-world uses for EVs. Figure 1 depicts the various types of EVs which are available in the global market. Clustering methods are employed to overcome power grid issues caused by electric vehicle growth [3]. It evaluates current

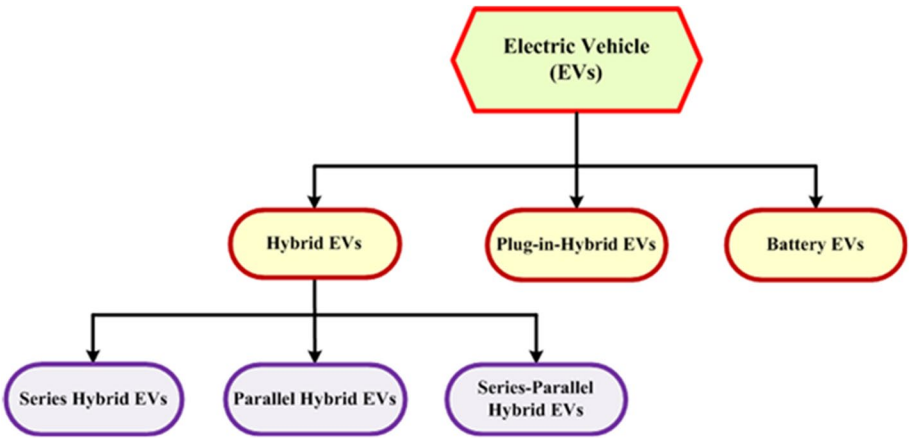

Fig. 1 Classification of EVs

approaches, examines user behavior, driving patterns, batteries, and charging stations, and offers study on distribution implications, emergency charging, rebate equity, and big data in transportation management. Analyzing user behavior and driving behaviors, clustering approaches help power networks integrate electric vehicles (EVs). Patterns in huge datasets help estimate charging requests and optimize grid management. Clustering allows infrastructure design by categorizing customers by billing choices and consumption patterns. Anticipating peak demands ensures effective distribution and reduces power system pressure. EV usage increases and clustering lets utilities respond to shifting needs, making power infrastructure more robust and sustainable. These methods improve EV incorporation with developing power networks. The article emphasizes the need for EV-grid integration optimization using electric vehicle behavior modeling. It provides insights and integration solutions for diverse circumstances with a complete model selection methodology [4]. In [5] discusses PV-grid charging profit potential, infrastructure, grid integration, economic constraints, capacity, and intermittency. A novel sliding mode controller (SMC) outperforms existing controllers in high-voltage power interface difficulties [6].

In [7] examines V2G bidirectional converter topologies for grid-to-EV battery energy transmission. Using a modified single-ended main inductor converter, a bidirectional battery charger charges 48 V and 120 V battery-powered automobiles effectively. Experimental findings show enhanced bidirectional operation and simpler switch ratings, improving performance and productivity [8]. Power factor correction, voltage regulation, and dynamic adaptation are implemented via an onboard charging unit with an adaptive sliding mode controller [9]. Genetic algorithms reduce chattering and improve parametric fluctuation adaptability by optimizing controller gains. MATLAB/Simulink simulations show that a state-of-charge-based high-level controller for smart V2G and G2V operations outperforms sliding mode and finite time synergetic control. A single-stage three-phase bidirectional AC-DC inductive power transfer converter for V2G applications [8] offers low input current distortion, high efficiency, output short-circuit protection, and soft-switching.

Literature review

In [10], a three-level dual-active-bridge converter for bidirectional EV charging is suggested with four modes of operation to accommodate a broad variety of EV voltages. Experimental data confirm its efficacy. Algorithms are employed to dynamically select the optimal operating mode in real time, reducing the transformer's RMS current in electric vehicle charging. Experimental results support the feasibility and advantages of the proposed dual-active-bridge (DAB) converter. In three-level DAB converter's four operating modes allow bidirectional EV charging at different voltages. The soft-switching dual-active-bridge converter has zero voltage, zero current, and combinations of these modes. The converter optimizes power transmission by matching the EV's voltage during unidirectional charging. In reverse power flow for vehicle-to-grid applications, the converter smoothly switches modes to accommodate EV battery voltage changes. This flexibility boosts converter efficiency and reduces switching losses. Soft-switching reduces electromagnetic interference, improving system dependability. These modes provide robust and adaptive bidirectional EV charging across varied voltage settings. In [11], introduce a fault-tolerant method for current-fed dual active bridge (CF-DAB) converters equipped with blocking capacitors. The approach addresses open-circuit and frozen-phase faults, providing practical and low-loss fault isolation and ensuring the dependability of multiphase converters [12] presents a cost-effective bidirectional off-board electric vehicle charger utilizing a multilevel topology and dual active bridge configuration.

It incorporates a novel control method involving synchronous reference frame control for active rectification and dual-phase shift control in the DC-DC stage to enable safe zero voltage switching operation. Optimal control settings are determined through particle swarm optimization. Simulations and a 3.3-kW laboratory prototype confirm the charger's performance under various voltage and loading conditions. In [13], a comprehensive design methodology for a resonant dual active bridge (R-DAB) converter tailored for Li-ion battery charging is introduced. The methodology optimizes resonant tank parameters using pulse frequency modulation and phase-shift modulation to minimize switching losses.

Contribution and paper organization

Validation through simulations and a 1 kW/30A laboratory prototype affirms the effectiveness of the dual control method and the proposed design approach [14] present a rapid phase-shift control approach for bidirectional dual active bridge (DAB) DC-DC converters, enhancing transient response during power-changing operations. By combining pulse-width modulation (PWM) with pulse frequency modulation (PFM), this method enables effective phase-shifting without causing DC imbalances or other adverse effects. This paper is to analyze and model the three-phase bidirectional charger which can operate in G2V and V2G mode. The main contributions of this paper are as follows:

- The charger module employs a two-stage power conversion process for efficient energy transfer or conversion, commonly used in modern charger designs.

- Advanced power converters are employed for improved efficiency and performance during the conversion stage, enhancing energy transfer and management.
- Simulation environments enable the observation of V2G (vehicle-to-grid) and G2V (grid-to-vehicle) charging effects and their impacts on power systems.

The current paradigm of electric vehicle (EV) integration with the grid demands efficient bidirectional power flow. However, conventional on-board chargers face challenges in achieving optimal vehicle-to-grid (V2G) and grid-to-vehicle (G2V) control. The soft-switching dual active bridge converter (SS-DAB) emerges as a promising solution. This research addresses the critical problem of enhancing bidirectional on-board charging for EVs, focusing on V2G and G2V control optimization. The aim is to develop an innovative SS-DAB-based charger system that optimally manages power flow in both directions, ensuring efficiency, reliability, and seamless integration between EVs and the grid. The main contribution lies in the soft-switching dual active bridge converter's advanced technology, enabling bidirectional power flow in on-board chargers for electric vehicles. This innovation enhances vehicle-to-grid (V2G) and grid-to-vehicle (G2V) control, optimizing energy transfer efficiency, reducing losses, and fostering a more resilient and integrated electric vehicle ecosystem. This paper is organized as follows: Ev's impact on the distribution grid and exploration of three-phase bidirectional charging is delved in the "Methods" section. Moving to the "Results and discussion" section, simulation results for the proposed SS-DAB-based bidirectional charger are detailed. Finally, the "Conclusions" section encapsulates the research work's summary.

Methods

According to [15], choosing an electric automobile (EV) battery is difficult. EVs cut urban pollution and operate quietly, making them a popular public transit option. Their environmental effect is negligible when fuelled by renewable energy or modern,

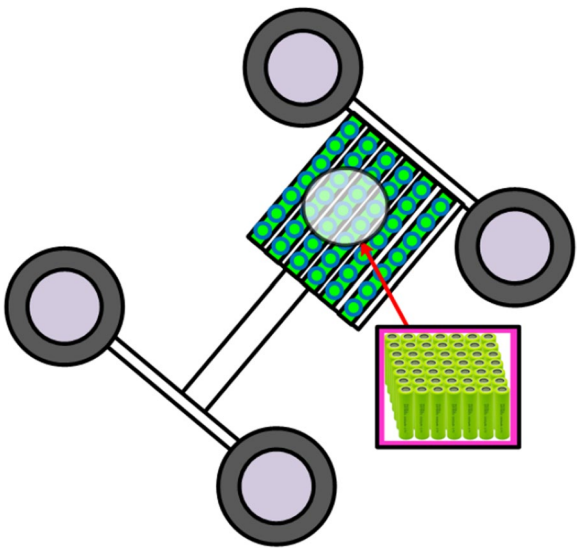

Fig. 2 Battery pack in EV

emission-controlled coal plants. EVs cost a third less to operate than combustion engine automobiles. Additionally, kinetic energy recovery systems boost efficiency. Figure 2 shows how non-linear least square regression estimates battery pack characteristics like open circuit voltage (OCV). The battery pack open circuit voltage can be defined as

$$OCV(X)_{Pack} = a_{01}\exp(-\frac{x-b_1}{c_1})^2 + a_{02}\exp(-\frac{x-b_2}{c_2})^2 + a_{03}\exp(-\frac{x-b_3}{c_3})^2 + a_{04}\exp(-\frac{x-b_4}{c_4})^2 \quad (1)$$

where, (a_{01}, a_{02}, a_{03}, b_1, b_2, b_3, c_1, c_2, and c_3) are estimated regression parameters, X is SoC. The measured part (y_i), and estimated value (y_i^I) of root mean square error (RMSE) and root mean square percentage error (RMSPE) were used to assess battery models. Equations (2) and (3) define RMSE and RMSPE.

$$RMSE = \sqrt{\frac{1}{k}\sum_{i=1}^{k}(y_i - y_i^I)^2} \quad (2)$$

$$RMSPE = \sqrt{\frac{1}{k}\sum_{i=1}^{k}\left(\frac{y_i - y_i^I}{y_i^I}\right)^2} \quad (3)$$

The RMSE and RMSPE of the battery voltage are 0.0328 V and 0.85% in the high SoC zone, and 0.0245 V and 0.61% in the low SoC region.

EV's impact on the distribution system

Transmission losses can be reduced by separating power production and distribution, however dispersed solar arrays change voltage and frequency. Since solar energy output fluctuates from 9 AM to 6 PM, feeder voltage might exceed acceptable values. To fix this, loads should use electricity during peak generation. Solar production normally increases from 9 to 10 AM, therefore EV charging coincides with this. Due to increased solar energy intake, feeder voltage rises. Optimal charging at peak solar generation between 10 AM and 12 PM reduces voltage oscillations. EV charging using extra solar power stabilizes feeder voltage. Maintaining EV charging from 12 to 2 PM uses high solar output to reduce feeder voltage swings. This noon-time has abundant sun energy. As solar output stays high between 2 and 4 PM, EV charging absorbs extra solar power to stabilize the system and avoid voltage spikes. Tapering EV charging from 4 to 6 PM matches declining solar input. Limiting feeder voltage fluctuations from peak solar output to lower levels is achieved by reducing solar generation gradually. Synchronizing EV charging with optimum solar output between 9 AM and 6 PM maximizes renewable energy use and reduces feeder voltage fluctuations. Electric vehicle (EV) charging patterns are unpredictable; thus, they must be aligned with peak generating periods. Smart grid technology, demand-side management, and enhanced control techniques reduce energy consumption, promote grid stability, and protect infrastructure during peak generation,

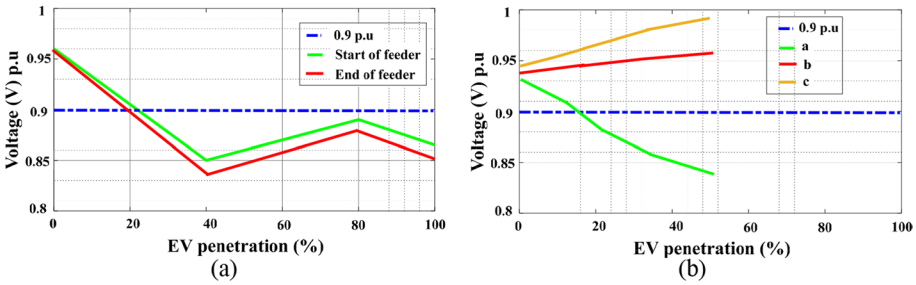

Fig. 3 EV penetration of **a** grid impedance and **b** phase interdependence

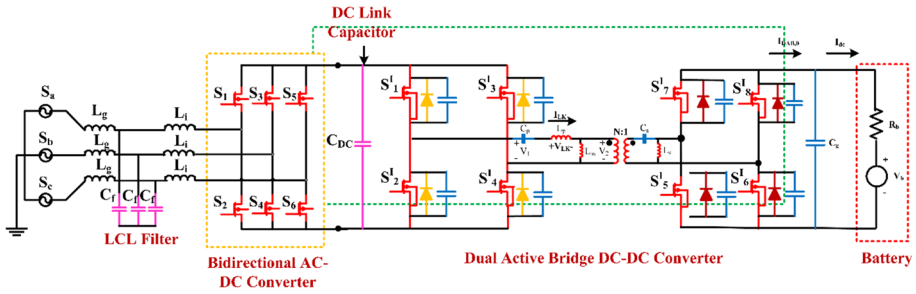

Fig. 4 Structure of three-phase battery charger

providing a smooth integration of renewables and EVs and avoiding voltage concerns [16].

Figure 3a shows that charging electric vehicles (EVs) during peak hours lowers line voltage, particularly as you go down the line. Smart charging and grid management solutions, especially in rural regions, are crucial to preventing power outages and network challenges during peak demand. In Fig. 3b, more EVs linked to phase a cause greater voltage drops than phases b and c. To balance phase-to-phase load, electric vehicles (EVs) must be used with bidirectional chargers. This transportation and energy transition greatly affects electric utility operations. As EV usage rises, grid support, demand response, and new business models give energy sector prospects. Grid management and infrastructure development are crucial to realizing this promise and transitioning to a sustainable and resilient energy system.

Three-phase bidirectional charger

Three-phase bidirectional charger design and grid integration control are covered in this section. EVs battery pack, three-phase AC, filter, AC-DC, and DC-DC converters make up the charger shown in Fig. 4. An AC-DC converter transports power from the AC supply to the DC bus, while a dq controller manages energy flow to the vehicle's battery pack for bidirectional energy exchange and grid integration.

AC-DC converter

A three-phase bidirectional AC to DC converter with switches S_1–S_6 properly converts AC power to DC for EV charging. This converter rectifies three-phase AC voltage while charging and gives extra power to the grid in vehicle-to-grid situations. A switching

sequence control method ensures accurate and efficient energy conversion. Flexible for EVs and grid integration, this bidirectional converter dynamically controls power flow to optimize charging, discharging, and renewable energy consumption. The switching function is defined by

$$S(t) = \begin{cases} 1; switchON \\ 0; switchOFF \end{cases} \tag{4}$$

Transistors and diodes behave as short circuits during conduction and open circuits during the blocking state. When switches are turned off, there is no tail current, and when diodes are reversed, there is no recovery current. Switches between the blocking and conducting phases are instantaneous. With a three-phase full-bridge in consideration, AC side current, *i*, is a DC quantity free of ripple throughout the switching cycle.

$$V_t = \frac{V_{dc}}{2}(2d - 1) \tag{5}$$

$$V_t = m\frac{V_{dc}}{2} \tag{6}$$

where d is the duty cycle, adjusting m from -1 to 1 causes a linear change in the average voltage at the AC-side terminal V_t, where m = 0 represents the zero averaged voltage. The Voltage Source Converter (VSC) is a frequency converter that is provided by the power provider and is required to be used. To restate this, the time and frequency sinusoids that are imposed by the grid serve as a representation of the three-phase values. Power systems depend on the Voltage Source Converter (*Vsc*) to manage DC voltage and real (P_s) and reactive (Q_s) powers. A true reactive power controller, it uses grid-imposed frequency. At the Point of Common Coupling (PCC), the VSC system optimizes P_s and Q_s transmission for fast response.

Industrial applications now employ voltage-mode control, which was formerly used in FACTS controllers. The AC-side terminal of the VSC may be adjusted for phase angle and voltage amplitude relative to the PCC voltage to precisely regulate P_s and Q_s. In the Voltage Source Converter (VSC), the phase angle and magnitude of the VSC line current relative to the Point of Common Coupling (PCC) voltage regulate real (P_s) and reactive (Q_s) powers. Modern EV chargers use current-mode control to improve VSC and AC system stability and dynamic performance. Figure 5 shows how a dq-frame current controller controls reactive and actual power. The d-q controller precisely controls Ps and Q_s by separating line current into i_d and i_q components. From altered feedback and feedforward signals, compensators create dq-frame control signals.

Phasor representation of space in dq frame

Consider the space phasor $f(t) = f_\alpha + f_\beta$ the d-q to α-β frame transformation is defined as

$$f_d + jf_q = \overrightarrow{f(t)}e^{-jp(t)} = (f_\alpha + f_\beta)\overrightarrow{f(t)}e^{-jp(t)} \tag{7}$$

Which is a phase shift in $\overrightarrow{f(t)}$ by -$\rho(t)$. The angle $\rho(t)$ can be chosen arbitrarily. However, if $\overrightarrow{f(t)} = f(t)e^{j(\omega t+\theta_0)}$ then choosing $\rho(t)$ equal to ωt results in space phasors

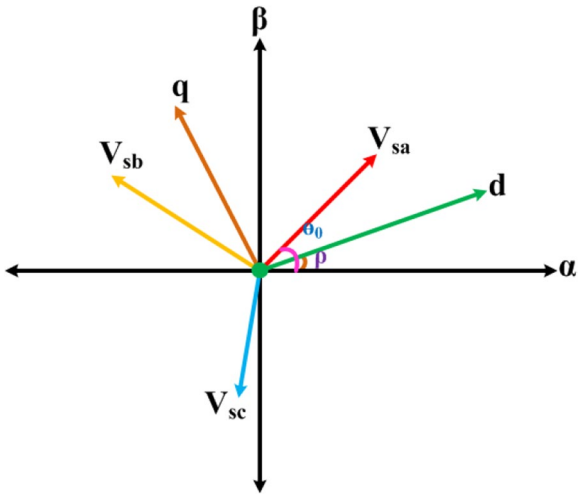

Fig. 5 Vector representation of PLL

$$f_d + jf_q = f(t)e^{j(\omega t+\theta_0)}e^{-j(\omega t)} \tag{8}$$

The inverse transformation is

$$\overrightarrow{f(t)} = f_\alpha + jf_\beta = (f_d + jf_q)e^{j\rho(t)} \tag{9}$$

When taken into consideration, the voltages of the three phases are as follows:

$$\left.\begin{aligned} V_{sa}(t) &= V_s\cos(\omega_0 t + \theta_0) \\ V_{sb}(t) &= V_s\cos(\omega_0 t + \theta_0 - \frac{2\pi}{3}) \\ V_{sc}(t) &= V_s\cos(\omega_0 t + \theta_0 - \frac{4\pi}{3}) \end{aligned}\right\} \tag{10}$$

where V_s is the line to neutral voltage peak value, θ_0 is the source starting phase angle, and ω_0 is the frequency of the AC system. The space-phasor equivalent of V_{sabc} is

$$V_s(t) = V_s e^{j(\omega_0 t+\theta_0)} \tag{11}$$

The dynamics of VSC are described by the following equation

$$L_f\frac{di}{dt} = -Ri + V_t - V_s \tag{12}$$

Substituting for V_s, then Eq. (13) becomes

$$L_f\frac{di}{dt} = -Ri + V_t - V_s e^{j(\omega_0 t+\theta_0)} \tag{13}$$

Then by using $i = i_{dq}e^{jp}$ and $V_t = Vs\, e^{j(\omega_0 t+\theta_0)}$ provides

$$L_f\frac{di_{dq}e^{j\rho}}{dt} = -Ri_{dq}e^{j\rho} + V_{tdq}e^{j\rho} - V_s e^{j(\omega_0 t+\theta_0)} \tag{14}$$

where $f_{dq}=f_d+jf_q$ and rewriting the above equation as

$$L_f\frac{di_{dq}}{dt}=-j(L_f\frac{d\rho}{dt}i_dq)-Ri_{dq}e^{j\rho}+V_{tdq}-V_se^{j(\omega_0t+\theta_0-\rho)} \tag{15}$$

The dq axis voltage equations are

$$\left.\begin{aligned}V_{sd}(t)&=V_s\cos(\omega_0t+\theta_0-\rho)\\V_{sq}(t)&=V_s\sin(\omega_0t+\theta_0-\rho)\end{aligned}\right\} \tag{16}$$

Phase-locked loop

The phase-locked loop (PLL) comprises essential components: the phase detector, low pass filter, and voltage controlled oscillator (VCO) as depicted in Fig. 6. Maintaining V_{sq} at zero is critical for synchronizing the dq-axis, achieved by modulating the dq-rotational frame's speed.

Ultimately, $\rho(t)=\omega_0(t)+\theta_0$ and $V_{sd}=V_s$. The VCO acts as a resettable integrator when its output reaches 2/pi, allowing precise synchronization. Bipolar sine triangle pulse width modulation generates pulses by comparing the carrier signal V_{tri} to the reference signal V_{sine}. PLL manages synchronization through V_{sdq} manipulation, pulse generation using bipolar sine triangle modulation, and VCO precision, vital for applications requiring synchronous dq-axis rotation, such as motor control and power electronics.

Soft-switching dual active bridge DC-DC converter

In EV bidirectional charging, the soft-switching dual active bridge (SS-DAB) DC-DC converter with two LLC filters provides constant and dependable performance throughout operating modes. It supports soft-switching, resonant operation, high-frequency isolation, voltage control, and efficiency improvement. Square wave outputs are produced by regulating main and secondary bridges concurrently with 50% duty cycle. Key qualities make the soft-switching dual active bridge (SS-DAB) DC-DC converter efficient for bidirectional EV charging. Its soft-switching reduces switching losses, improving efficiency. Second, the converter's zero-voltage and zero-current switching modes maintain performance under different load circumstances. Two LLC filters reduce high-frequency components' electromagnetic interference and improve dependability. Both EV charging and discharging are stable with this dual-filter arrangement. Flexible operating modes and LLC filters make the SS-DAB efficient and reliable in bidirectional EV

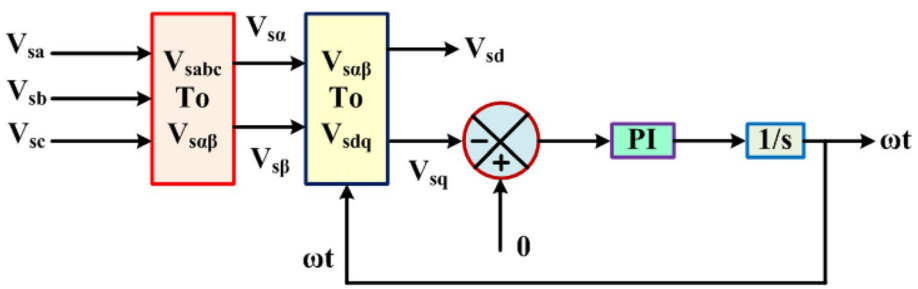

Fig. 6 Phase-locked loop

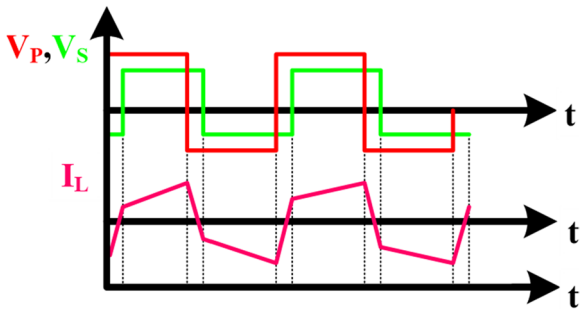

Fig. 7 Transformer primary and secondary voltages, inductor current

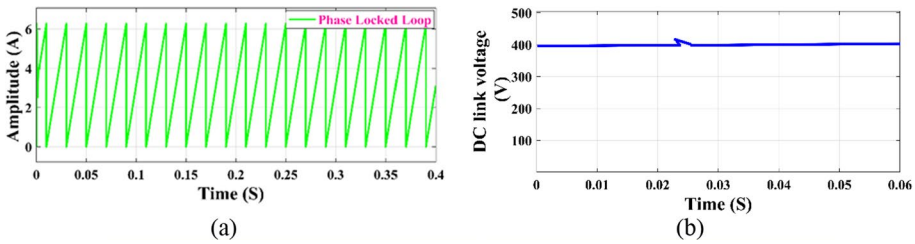

Fig. 8 **a** PLL tracking grid frequency, **b** dynamics of DC link voltage in V2G and G2V

charging situations, meeting electric vehicle power system needs. Figure 7 shows that inductor current and voltage waveforms split the switching pattern into four time periods. Dual active bridge (DAB) converters measure primary and secondary voltages across the transformer's main and secondary windings, respectively. In Fig. 7, the transformer turns ratio (Np/Ns) is the primary-to-secondary turn ratio. The square root of the primary-to-secondary voltage ratio. This turn ratio affects voltage transformation and may determine DAB converter output voltage, affecting power conversion efficiency and performance.

Results and discussion

A simulation scenario is used to evaluate the charger's operation and grid compliance as utility-level circumstances cannot be replicated in real time. PLL is used to synchronize a locally produced signal with the grid frequency signal. The charger performs when the DC-link voltage decreases to 400 V in the simulation as shown in Fig. 8a–b. While this study focuses on $V_{dc}=400$ V, the results provide light on the charger's grid compliance and synchronization at other voltage levels. It is essential to examine the charger's utility compliance and grid interconnection capability. Figure 9a shows that the DC-Link voltage was in the V2G mode between 0 and 1 s when the soft-switching dual active bridge (SS-DAB) DC-DC converter was operating. The voltage difference facilitates power exchange between the DC-DC converter and AC-DC converter.

From 1 to 2 s, it transitions to G2V operation, functioning as a buck converter, and power exchange occurs in Fig. 9b. The dual LCL filter ensures smooth grid voltage and current Fig. 9c, nearly in phase with the grid voltage, achieving a near-unity power factor. Figure 9d illustrates the inverter terminal voltage and inverter-side current with ripples at the AC-DC converter's switching frequency, characteristic of the SS-DAB DC-DC

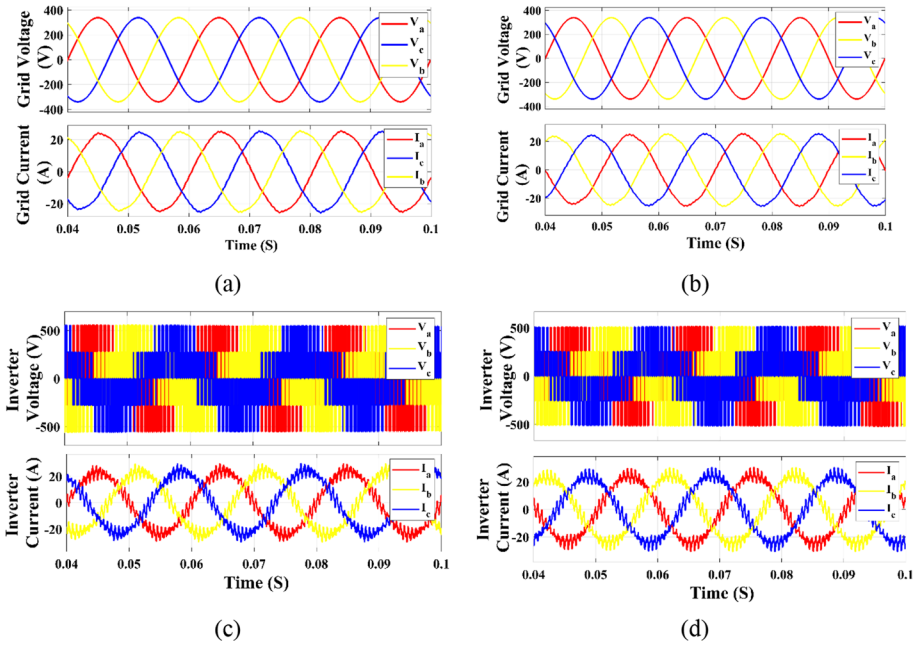

Fig. 9 Simulation results of **a** grid voltage and current in V2G, **b** grid voltage and current in G2V, **c** inverter voltage and current in V2G, and **d** inverter voltage and current in G2V

converter's soft-switching operation. Switching waveforms are used to analyze the dual active bridge (SS-DAB) DC-DC converter's soft-switching capability for inverter terminal voltage and current ripples at the switching frequency. Soft-switching occurs when switches alternate on and off with low voltage or current spikes. The inverter terminal voltage and current waveforms indicate soft-switching features and decreased switching losses. The converter's performance must be assessed to ensure effective power transmission with low high-frequency ripples. This confirms the converter's ability to facilitate bidirectional power flow with reduced switching losses, ensuring efficient energy exchange in both vehicle-to-grid (V2G) and grid-to-vehicle (G2V) modes. Although it operates in V2G mode, the soft-switching dual active bridge converter-based bidirectional on-board charger can keep fine control over the characteristics of the battery. A steady battery voltage is maintained by the system, which optimizes it for effective power exchange. At the same time, the system carefully regulates the flow of current to guarantee dependability and performance, which ultimately improves the overall functioning of electric vehicles within the grid.

In grid-to-vehicle (G2V) mode, the soft-switching dual active bridge converter (SS-DAB) based bidirectional on-board charger maintains efficient power transfer. The battery experiences a stable voltage of 400 V and a controlled current of 50A, ensuring optimal charging. This configuration enhances charging performance, minimizing energy loss and optimizing electric vehicle (EV) integration with the grid. Modulation signals (m_d and m_q) in the dq-axis are converted to abc form to create a sinusoidal AC signal. Pulses from Sine Triangle Pulse Width Modulation control the switches. Figure 10 shows Bipolar Sine Triangle Pulse Width Modulation comparing the carrier signal (V_{tri}) to the reference signal (V_{sine}).

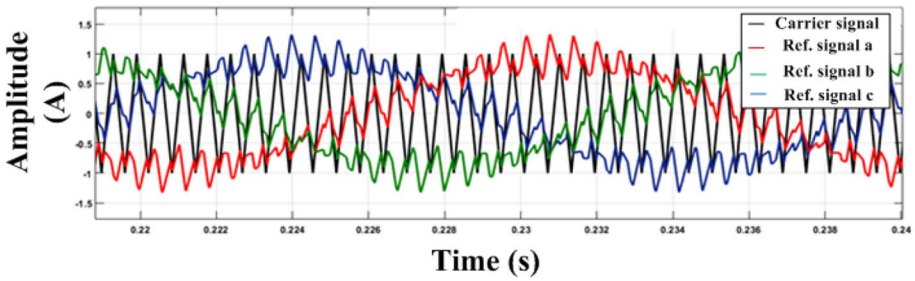

Fig. 10 Carrier signal and modulated reference signal

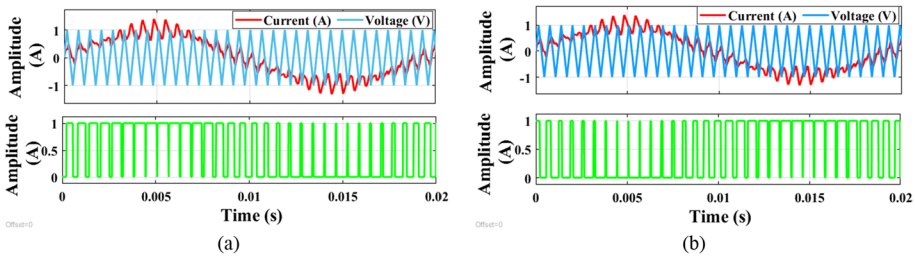

Fig. 11 **a** Bipolar SPWM for S_1 of phase-a, **b** bipolar SPWM for S1 of phase-b

In the Sine Triangle Pulse Width Modulation technique, a pulse is generated when the sinusoidal reference signal (V_{sine}) exceeds the triangular carrier signal (V_{tri}). This pulse is then sent to one switch in the leg, while its complementary pulse is sent to the other switch. This process creates a modulated waveform. The resulting pulse train controls the operation of the switches in the power converter. A 180-degree phase shift in the current, typical for PWM applications, is essential for proper converter operation and achieving bidirectional power flow. Figures 11a and b depict the modulating signals and carrier signals, providing a comprehensive overview of their interaction. The modulating signals dictate when the power switches should be turned on or off, using the carrier signal as a reference for switching timing. Figures 12a and b illustrate the State of Charge (SoC) fluctuations during discharge and charge modes of the battery. In the discharge mode, as energy is released, SoC decreases from 50 to 49.996%. The constant discharge rate of 4.5A corresponds to a voltage drop from 400 to 376 V, aligning with the decreasing SoC.

Conversely, in the charge mode, SoC increases as the battery receives energy. The steady charging rate of 0.55 A leads to a voltage rise from 384 to 396 V, reflecting the growing battery capacity percentage. This behavior continues with a constant charging rate of 0.125A, resulting in voltage increasing from 394 to 396 V. Figure 12c provides insight into the power flow process. The active power supplied to the grid indicates the actual power transferred, contributing to total energy exchange. Simultaneously, the dual LCL filter consumes minimal reactive power. Reactive power is essential for voltage regulation and overall power system stability. The given system conforms to the fundamentals of PWM control, which enables accurate regulation of the flow of power. The fact that the battery and the grid engage in a two-way exchange

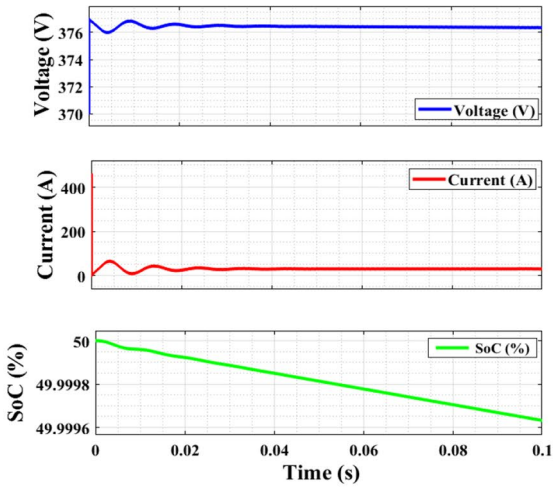

(a)

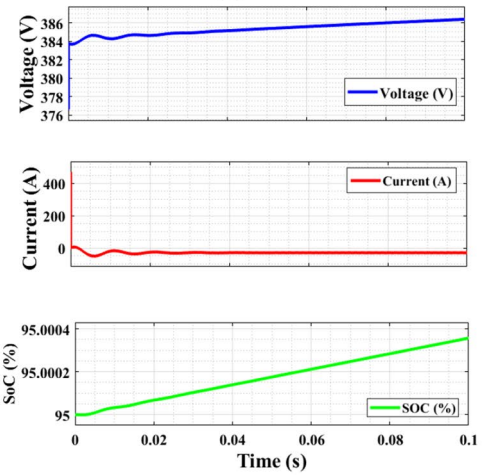

(b)

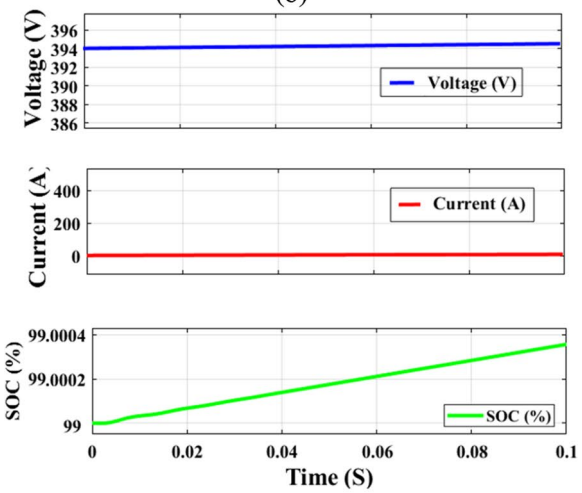

(c)

Fig. 12 **a** Battery voltage, current, and SoC in V2G mode in CC. **b** Battery voltage, current, and SoC in G2V mode in CC. **c** Battery voltage, current, and SoC in charge mode in CC

Table 1 EV battery specifications

Parameter	Value
Voltage	400 V
Battery pack efficiency	> 95%
Energy Capacity (kWh)	6.6
Max Power (kW)	3.5
Current	8.75 A

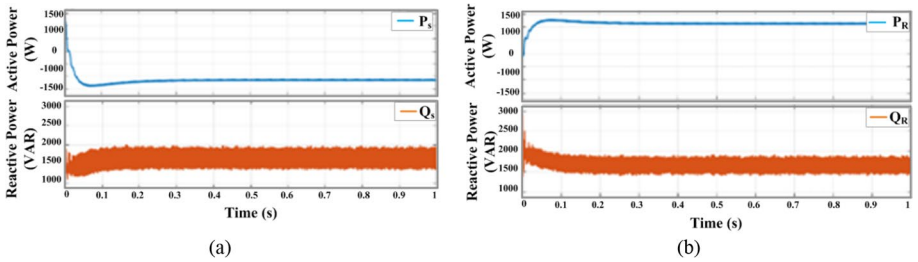

Fig. 13 **a** Active, reactive power in V2G. **b** Active, reactive power in G2V

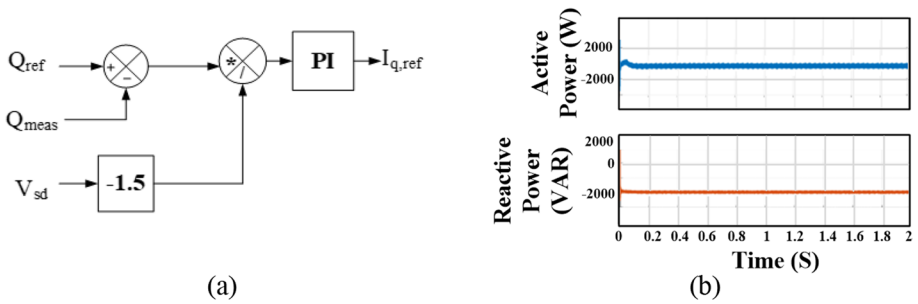

Fig. 14 **a** Q compensation and **b** Q compensation — grid voltage and current

of power is reflected in the way that SoC fluctuates while switching between various modes. The electrical specifications of EV battery can be observed in Table 1.

Figure 13a and b illustrate the active power and minimal reactive power drawn from the grid during V2G and G2V modes. The dual LCL filters consume only a small amount of reactive power. In Fig. 14a, voltage and current levels when EVs contribute reactive power to the grid are shown. A higher current voltage than grid voltage indicates the EV as the source of grid reactive power. Figure 14b displays the delivery of reactive power to the grid. The charging process can be optimized by using multistage constant current charging, which avoids the less efficient CC-CV charging method, where the remaining 20% of battery capacity is charged slowly in the CV mode after an 80% CC charge.

Conclusions

This research provides a powerful three-phase bidirectional charger that incorporates a battery pack, an AC-DC converter, and a DC-DC converter that is equipped with a soft-switching dual active bridge (SS-DAB). Both grid-to-vehicle (G2V) and vehicle-to-grid (V2G) situations can benefit from the use of a unified Voltage Source Converter

(VSC) control technique, which guarantees efficient power transfer. It is important to note that the charger's design enables it to function in all four operating quadrants, which provides adaptability. The results of the simulation validate the proposed unified system controller by demonstrating rapid dynamic response, excellence in steady-state functionality, and resilience to fluctuations in grid demand. This highlights the relevance of the SS-DAB-based Bidirectional On-Board Charger in promoting the integration of electric vehicles in a manner that is both effective and friendly to the grid.

The proposed SS-DAB bidirectional charger topology enhances efficiency, reducing power losses during bidirectional energy transfer. The SS-DAB enables a seamless transition between charging and discharging modes, optimizing energy flow. With soft-switching capabilities, it minimizes switching losses, enhancing overall converter efficiency. The converter's flexible control facilitates precise regulation of power flow, ensuring grid stability.

Abbreviations

DAB	Dual active bridge
SS-DAB	Soft-switching dual active bridge
EV	Electric vehicle
CF-DAB	Current fed dual active bridge
R-DAB	Resonant dual active bridge
PFM	Pulse frequency modulation
OCV	Open circuit voltage
RMSE	Root mean square error
RMSPE	Root mean square percentage error
VSC	Voltage Source Converter
PCC	Point of Common Coupling
PLL	Phase-locked loop
VCO	Voltage control oscillator

Acknowledgements
Not applicable.

Authors' contributions
JVG Rama Rao prepared manuscript preparation, writing, and results editing, S. Venkateshwarlu analyzed data collection, manuscript editing, manuscript sketch work, and software simulation work. All authors read and approved the final manuscript.

Funding
There is no funding body involved in this article.

Availability of data and materials
Figures: Microsoft Visio 2007, Microsoft Excel, Tables: Microsoft Word, Simulation Software: MATLAB/Simulink.

Declarations

Ethics approval and consent to participate
We declare that this manuscript is original, has not been published before, and is not currently being considered for publication elsewhere and there are no conflicts of interest for this publication. As the corresponding author, we confirm that the manuscript has been read and approved for submission by all the named authors.

Competing interests
There are no competing interests involved in this manuscript/article.

Received: 2 November 2023 Accepted: 1 February 2024
Published online: 21 February 2024

References

1. Guo X, Sun Y, Ren D (2023) Life cycle carbon emission and cost-effectiveness analysis of electric vehicles in China. Energy Sustain Dev 72:1–10. https://doi.org/10.1016/j.esd.2022.11.008

2. Tang B, Xu Y, Wang M (2022) Life cycle assessment of battery electric and internal combustion engine vehicles considering the impact of electricity generation mix: a case study in China. Atmosphere (Basel) 13(2). https://doi.org/10.3390/atmos13020252
3. Ismail AA, Mbungu NT, Elnady A, Bansal RC, Hamid A-K, AlShabi M (2023) Impact of electric vehicles on smart grid and future predictions: a survey. Int J Model Simul 43(6):1041–1057
4. Cao C, Wu Z, Chen B (2020) Electric vehicle-grid integration with voltage regulation in radial distribution networks. Energies 13(7):1–18. https://doi.org/10.3390/en13071802
5. AJ Alrubaie AJ Alrubaie, Salem M, Yahya K, Mohamed M, Kamarol M (2023) A comprehensive review of electric vehicle charging stations with solar photovoltaic system considering market, technical requirements, network implications, and future challenges. Sustain 15(10). https://doi.org/10.3390/su15108122
6. Waghmare T, Chaturvedi P (2023) Sliding mode controller for multiphase bidirectional flyback converter topology in hybrid electric vehicle applications. Energy Rep 9:40–47. https://doi.org/10.1016/j.egyr.2023.05.051
7. Panchanathan S et al (2023) A comprehensive review of the bidirectional converter topologies for the vehicle-to-grid system. Energies 16(5). https://doi.org/10.3390/en16052503
8. Yuan J, Dorn-Gomba L, Callegaro AD, Reimers J, Emadi A (2021) A review of bidirectional on-board chargers for electric vehicles. IEEE Access 9:51501–51518. https://doi.org/10.1109/ACCESS.2021.3069448
9. Lu Z, Zhang X (2022) Composite non-linear control of hybrid energy-storage system in electric vehicle. Energies 15(4). https://doi.org/10.3390/en15041567
10. Xuan Y, Yang X, Chen W, Liu T, Hao X (2019) A three-level dual-active-bridge converter with blocking capacitors for bidirectional electric vehicle charger. IEEE Access 7:173838–173847. https://doi.org/10.1109/ACCESS.2019.2957022
11. Zhang L, Y Wang Y Wang, L Cheng L Cheng, W Kang W Kang (2023) A three-parameter adaptive virtual dc motor control strategy for a dual active bridge dc–dc converter. Electron 12(6). https://doi.org/10.3390/electronics12061412
12. Naik N, Vyjayanthi C, Modi C (2023) Filter-based active damping of dab converter to lower battery degradation in ev fast charging application. IEEE Access 11:74277–74289. https://doi.org/10.1109/ACCESS.2023.3295988
13. Wu X, Zhang Y, Yang J (2022) Neutral-point voltage balancing method for three-phase three-level dual-active-bridge converters. Energies 15(17):6463. https://doi.org/10.3390/en15176463
14. Boya AK, Jyothi B (2023) A novel quadruple active bridge dc converter with reduced inductor current for ev battery charging. Adv Electr Electron Eng 21(2):92–106. https://doi.org/10.15598/aeee.v21i2.4646
15. Youssef R, Kalogiannis T, Behi H, Pirooz A, Van Mierlo J, Berecibar M (2023) A comprehensive review of novel cooling techniques and heat transfer coolant mediums investigated for battery thermal management systems in electric vehicles. Energy Rep 10:1041–1068. https://doi.org/10.1016/j.egyr.2023.07.041
16. Cha H, Chae M, Zamee MA, Won D (2023) Operation strategy of EV aggregators considering EV driving model and distribution system operation in integrated power and transportation systems. IEEE Access 11:25386–25400. https://doi.org/10.1109/ACCESS.2023.3251356

Publisher's Note